Julia Kelly   22nd March 2017

Short Term Scientific Mission Report

COST action OPTIMISE: ES1309

STSM applicant: Julia Kelly, Department of Geography, Swansea University, UK
STSM topic: Developing a methodology for combining UAV and ground-based multispectral imagery with carbon flux data in a boreal mire
STSM reference number: COST-STSM-ECOST-STSM-ES1309-090217-082691
STSM type: Regular (from United Kingdom to Sweden)
Period: 09/02/2017 to 05/03/2017
Host: Lars Eklundh, Department of Physical Geography and Ecosystem Science, Lund University, Sweden

1. Purpose of the STSM

The aim of the STSM was to support my PhD research by providing access to equipment for radiometric and geometric calibration of a FLIR Vue Pro 640 thermal infrared camera. The FLIR Vue Pro will be mounted on a PitchUp quadcopter UAV and flown regularly over the field site at Skogaryd Research Station (Sweden). The mission also provided an opportunity to acquire skills in UAV thermal imagery processing in Agisoft Photoscan Pro and a visit to Skogaryd Research Station. The high spatial resolution images from the UAV will be combined with data from ground-based sensors to produce high resolution, dynamic maps of the vegetation at the field site. These will then provide a basis for assessing the relationships between carbon fluxes measured at the site (with an eddy covariance flux tower) and spectral indices from the vegetation maps.

2. Description of the work carried out during the STSM

The work carried out during the STSM was divided into four parts:
  i.   Radiometric calibration of the FLIR Vue Pro 640
        a. Assessing the stabilization time of the camera
        b. Generating blackbody calibration curves for the camera
        c. Assessing the effect of wind and heating on the camera
        d. Assessing sensor noise
 ii.   Geometric calibration of the FLIR Vue Pro 640
iii.   Image processing in Agisoft Photoscan Pro
 iv.   Visit to the field site at Skogaryd Research Station

2.2 Radiometric calibration of the FLIR Vue Pro 640

The equipment setup for the radiometric calibration experiments is illustrated in Figure 1, with an example image of the blackbody radiator in Figure 2. A blackbody radiator (emissivity: 0.992) was placed 32cm away from the camera so that the entire device was visible in the field of view of the camera. A PT100 resistance thermometer recorded the temperature of the blackbody radiator every second. The camera was mounted on a tripod, with a copper-constantin thermocouple attached to the top surface of the camera case recording its temperature every second. A Kestrel 4500 pocket weather monitor recorded air temperature, relative humidity and wind speed every 30 seconds.

2.2.1   Assessing camera stabilization time

The purpose of the experiment was to assess the length of time required for the camera to produce stable image values after switch on. The camera was switched on and recorded images of the blackbody radiator every 30 seconds for 2 hours. The blackbody radiator maintained a constant temperature at 18.4°C (σ=0.2°C). To assess the change in camera raw signal over time, a circular area representing the centre of the blackbody was selected for all images. The same circle was used for all images and covered 33% of the total number of pixels in an image. The mean digital number value of all pixels within this circle was calculated for each image and plotted over time.

2.2.2   Blackbody calibration curve generation

The FLIR Vue Pro 640 is not radiometric therefore it was essential to generate calibration curves to model the relationship between camera raw signal and observed temperature. The blackbody radiator was cooled in an incubation chamber overnight (Conviron CMP4030) at 4°C (the minimum temperature of the chamber). Using the incubation chamber enabled the blackbody to be cooled without damage due to condensation. The minimum temperature reached by the blackbody was 6.5°C. Prior to removing the blackbody from the chamber, the camera is switched on and allowed to stabilize for 1 hour. After stabilization of the camera, the blackbody was placed 32cm way from the camera. The temperature of the blackbody was increased in 5°C steps (6.5°C, 10°C, 15°C, 20°C, 25°C, 30°C, 35°C, 40°C). The camera recorded 20 images of the blackbody at each temperature interval. During the experiment, room temperature was stable at 20.6°C (σ=0.3°C).

The same experiment was repeated by placing the camera and blackbody inside the incubation chamber which maintained air temperature at 10°C to investigate how camera temperature affects observed temperature. The blackbody was cooled overnight in the chamber at 10°C and reached a minimum temperature of 10.3°C. The camera was switched on and placed in the chamber where it was stabilized for 1 hour prior to the start of the experiment. The temperature of the blackbody was then increased in 5°C temperature steps (10.3°C, 15°C, 20°C, 25°C). The maximum temperature attainable by the blackbody in the chamber was 25°C at the maximum voltage supplied by its power source. The temperature of the chamber was stable at 10.8°C (σ=0.1°C) during the experiment.

Image processing for both experiments followed the same method as described in section 2.2.1. Standard deviation of the digital number values was also calculated for each temperature step.

2.2.3   Assessing the effect of wind and heating on the camera

An experiment was performed to test the influence of wind and external heating on camera performance, mimicking windy conditions and the effects of direct sunlight on the camera during UAV flight. The camera was switched on and stabilized for 1 hour prior to the start of the experiment. The camera was recording images of the blackbody every 30 seconds. A fan was placed 50cm away from the blackbody and camera to blow wind on the camera. The Kestrel 4500 pocket weather monitor was fixed on a clamp opposite the fan to record air temperature, humidity and wind speed. After the camera had stabilized, the fan was set to its lowest speed setting (2.0m/s, σ=0.2m/s wind speed) for 30 minutes. The fan was then switched off and the camera allowed to stabilize for 1 hour. Next the fan was switched to its highest speed setting (3.3m/s, σ=0.2m/s wind speed) for 30 minutes. The camera was then allowed to stabilize for 1 hour. The fan speed used is comparable to the speed at which the UAV is flown

(<5m/s). A control period of 30 minutes when the camera continued recording images of the blackbody without any wind or heating effect. Finally, a 500W halogen lamp was placed several centimeters above the camera to heat it. The camera was heated until it reached 45°C (5°C below the maximum operating temperature of the camera). The lamp was then turned off to avoid overheating the camera, and the camera continued recording images of the blackbody for 30 minutes. Image processing followed the same method as described in section 2.2.1.

2.2.4   Assessing sensor noise

An experiment was performed to test for noise between pixels on the sensor array and between images over time. The camera was moved closer to the blackbody radiator (8cm apart) so that the blackbody radiator entirely filled the field of view of the camera. In this way, each pixel on the camera sensor should have recorded the same temperature. The camera was switched on and stabilized for 1 hour prior to the start of the experiment. The blackbody temperature was stable at 19.1°C (σ=0.1°C). After stabilization, the frame rate of the camera was increased to record one image every second for 30 minutes (1800 images captured). Operating at a higher frame rate mimicked the conditions during UAV flight when the camera is recording images very frequently.

The frequency and strength of temporal noise affecting the camera was determined following the method outlined by Aubrecht et al. (2016). First, the mean of each pixel across all images was calculated and subtracted from the value of the pixel for each image. This produced the deviation from the mean pixel value for each pixel across all images. Next, the mean of all pixel deviations from the mean was calculated for each image. The image mean was then Fourier transformed to produce a power density spectrum. The plot shows the contributions of different frequency components to the mean image signal, whereby frequencies with higher powers contribute more significantly than those at lower powers.

To determine the spatial noise affecting the sensor, two analyses were performed. Thermal cameras with wide angle lenses are prone to 'vignetting' whereby pixels at the edges of the sensor record lower values than those at the centre when observing a surface of uniform radiance (Meier et al., 2011). To test for this effect, the mean digital number value recorded by each pixel across all images was calculated. The mean value of each pixel ('pixel mean') was then compared to the mean value of all pixels across all images ('image mean'). The sensor layout was plotted, with the colour of each pixel representing the relationship between the pixel mean and image mean. The final plot thus shows the mean deviation of each pixel from the image mean (variation across spatial area of the sensor).

Non-uniformity noise patterns, which appear as horizontal and/or vertical stripes across an image, may also be present in images recorded by thermal cameras (Aubrecht et al., 2016; Goodall et al., 2016). Following the method of Aubrecht et al. (2016), the mean value of all pixels across an image was subtracted from the image and this process was repeated for every image recorded. The deviation of each pixel from the image mean over time was then correlated to the deviation of the centre pixel from the image mean over time (i.e. across all images recorded). The correlation coefficients where then plotted for each pixel in their respective locations across the sensor to show whether neighbouring pixels exhibit similar behaviour (as would be expected if striped patterns were present on the sensor).

2.3 Geometric calibration of the FLIR Vue Pro 640

Geometric calibration of the camera was performed to provide information on camera intrinsic parameters to aid orthomosaic construction in Agisoft Photoscan Pro. A calibration target visible in the thermal infrared spectrum was constructed using a sheet of glass (Figure 3). Glass was chosen due to its thermal inertia which aids the generation of an evenly heated surface. A checkerboard pattern was drawn onto the glass with 50mm squares. White squares were painted with matt white paint which has a high emissivity (~0.95; Minkina and Dudzik, 2009). Black squares were painted with reflective aluminium rim paint which has a lower emissivity (~0.6; M. Mölder, personal communication, 24 February). The target was heated for at least 30 minutes with a 500W halogen lamp. The target was placed in a fixed position on the floor while the camera was held 2m above the target (to account for the hyperfocal distance and depth of field of the camera, while ensuring the target filled ~20% of the camera's field of view). Images of the target were captured from different angles, then processed using the Camera Calibration App, part of the Computer Vision System Toolbox, in MATLAB. The 20 images with the lowest reprojection errors (mean: 0.28 pixels) were chosen to calculate the camera intrinsic parameters.

2.4 Image processing in Agisoft Photoscan Pro

Lund University provided access to a dedicated workstation for running Agisoft Photoscan Pro, the software used to create orthomosaics from UAV imagery. Drawing on the expertise of staff and students at the university, I acquired knowledge of the workflow and data input requirements for processing images from UAV-borne sensors. The aim was to produce an orthomosaic with images from the FLIR Vue Pro from a test flight over the study area. Since the camera uses a narrow range of digital number values, all the images appear completely black when loaded into Photoscan. It is therefore necessary to rescale the images in order to detect features and label ground control points (although the software itself is able to produce an orthomosaic without rescaling). A rescaling method was developed in MATLAB using the imadjust function. The minimum and maximum digital number value across all images from one flight mission were calculated and used as an input to the function. In MATLAB, the images are processed as unsigned 16-bit integers, therefore the imadjust function rescales the pixel values to fill the 0-65535 range of values for a 16-bit integer. The images can then be loaded into Photoscan and any ground control points or other features can be identified. Once an orthomosaic is constructed, it could be opened in MATLAB and the reverse imadjust function applied to scale the digital numbers back to their original values. The reverse function was not tested as it was not possible to generate the orthomosaic from the available imagery. It will be tested as soon as an orthomosaic can be generated from images taken with the FLIR Vue Pro.

2.5 Visit to the field site at Skogaryd Research Station

A visit to the field site at Skogaryd Research Station was conducted between 17th - 19th February. I met with the field station manager and technicians to discuss the installation of new equipment for future UAV flight campaigns and a ground-based thermal camera. The field site is located in central Sweden (58° 23'N, 12° 09'E) and is part of SITES (Swedish Infrastructure for Ecosystem Sciences). The field site is an open minerotrophic mire ecosystem composed of patches of heather (*Calluna vulgaris*), White Beak-sedge (*Rhynchospora alba*) and several types of *Sphagnum* species. The mire is surrounded by Scots pine (*Pinus sylvestris*) and there is a sparse distribution of dwarf birch (*Betula nana*) across drier patches of the mire.
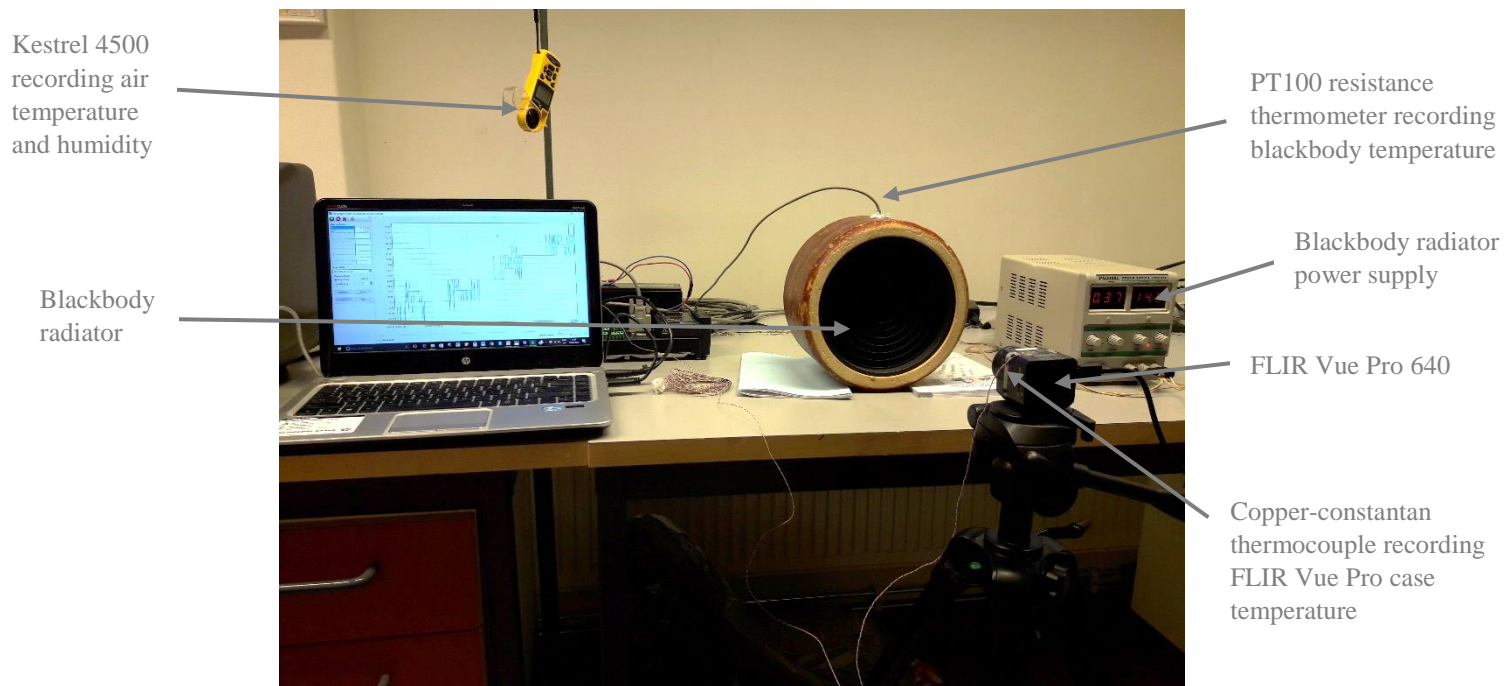
Figure 1. Photo of experimental setup and equipment for radiometric calibration of FLIR Vue Pro.
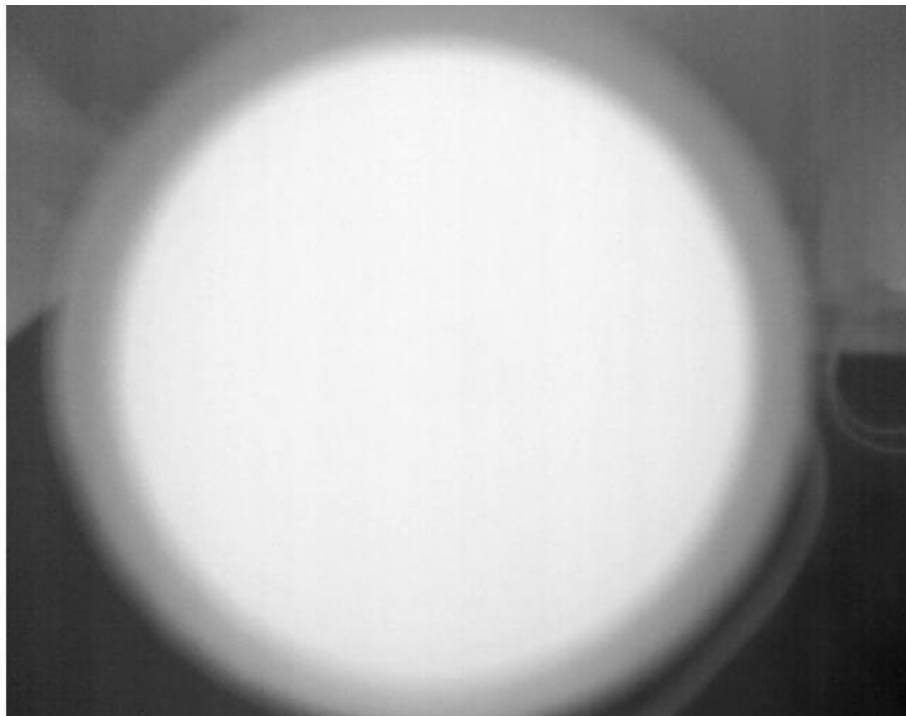

Figure 2. Image of the heated blackbody recorded by the FLIR Vue Pro during radiometric calibration. Only the central part of the image depicting the centre of the blackbody was used to generate the relationship between camera raw signal and observed temperature.
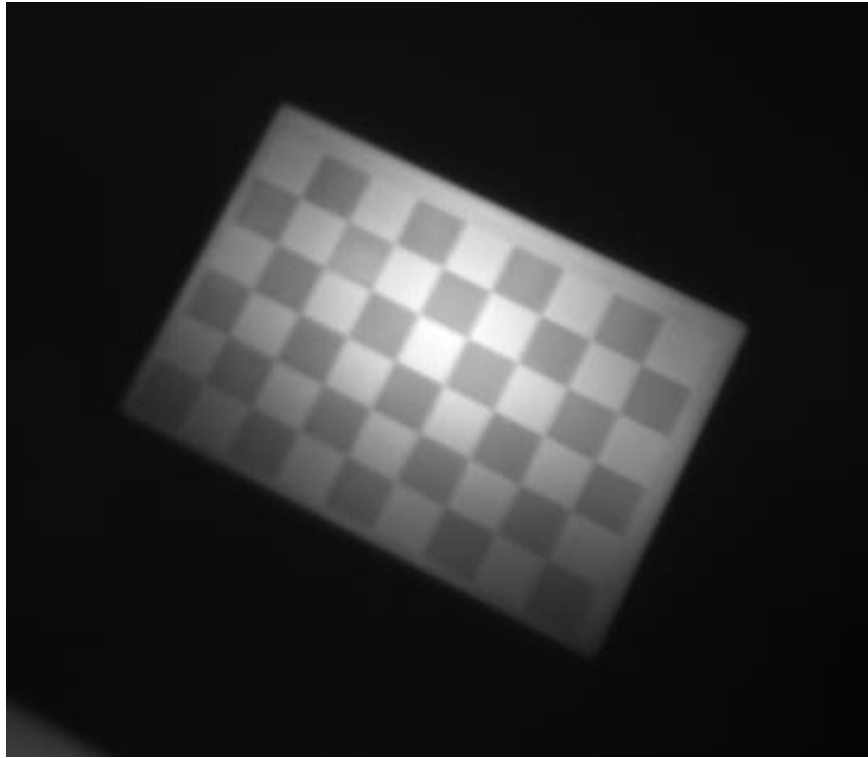
Figure 3. Geometric calibration target imaged with the FLIR Vue Pro.

3.   Description of the main results obtained

3.1 Radiometric calibration of the FLIR Vue Pro 640

3.1.1   Assessing camera stabilization time

The camera experienced significant fluctuations in raw signal output during the first 15 minutes of operation and required approximately 1 hour to fully stabilize (Figure 4). The experiment was repeated and produced the same results. It is recommended the camera is switched on at least 15 minutes prior to a UAV flight campaign to account for the most significant fluctuations in the camera signal.
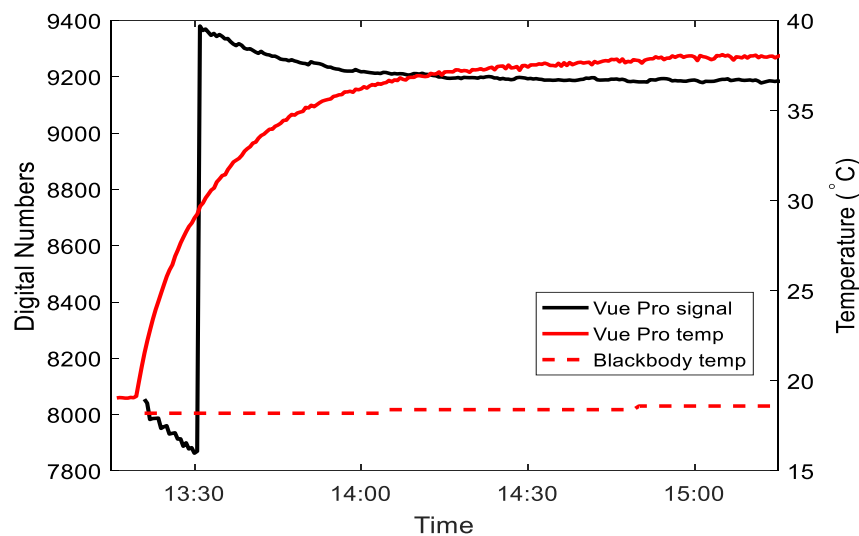

Figure 4. FLIR Vue Pro raw signal (digital numbers) over 2 hours after camera switch on.

3.1.2   Blackbody calibration curve generation

The calibration curves generated at room temperature (camera temperature = 38°C) and in the incubation chamber (camera temperature = 20°C) are shown in Figure 5. The camera raw signal has a linear response to observed temperature. The camera uses a narrow range of digital number values (FLIR Vue Pro records 14-bit images which range between 0-16383 digital numbers). Furthermore, the average image signal varies little between frames at each temperature step (σ <4 digital numbers for all temperature steps recorded) suggesting the camera is sensitive to <1°C temperature changes. However, the observed temperature is clearly affected by the temperature of the camera itself, with lower camera temperature associated with lower digital numbers at a given observed temperature.
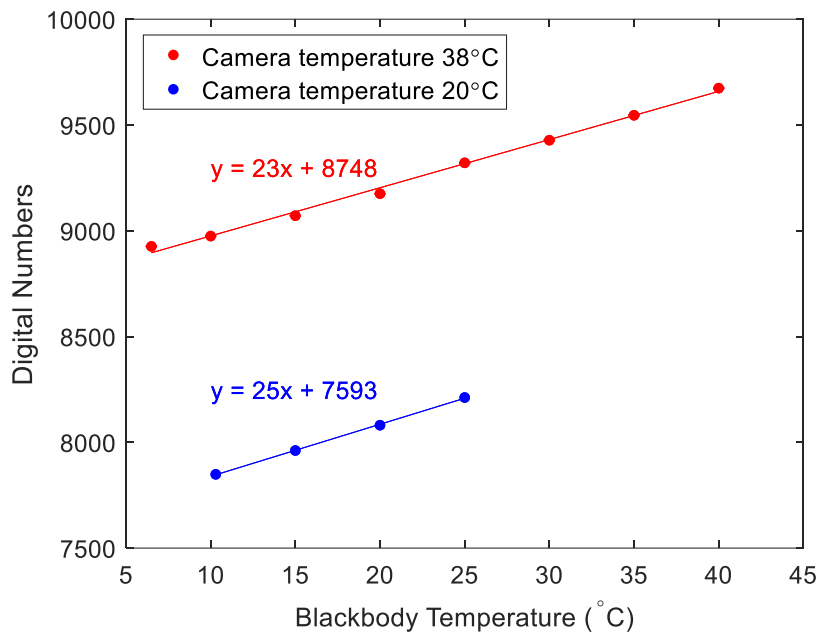

Figure 5. Blackbody calibration curves of FLIR Vue Pro 640 showing blackbody temperature on the x-axis and camera raw signal on the y-axis. Calibration curves were performed at two camera temperatures. Error bars are standard deviation of raw camera signal but are very small (>4 digital numbers).

3.1.3   Effect of wind and heating on the camera

Figure 6 shows the results of the experiment testing the effect of wind and heating on camera performance. There were large fluctuations in camera raw signal during each treatment, equivalent to up to ~18°C change in observed temperature by the camera. It was therefore difficult to determine a clear relationship between camera temperature and measured signal that could be used to correct for the influence of wind and heating on the camera. In this experiment, camera temperature is negatively related to camera signal, whereas the calibration curve experiment showed the opposite. It may be due to an overcompensation by the camera's

internal autocalibration mechanism as a result of the sudden change in camera temperature during the wind and heating experiment.
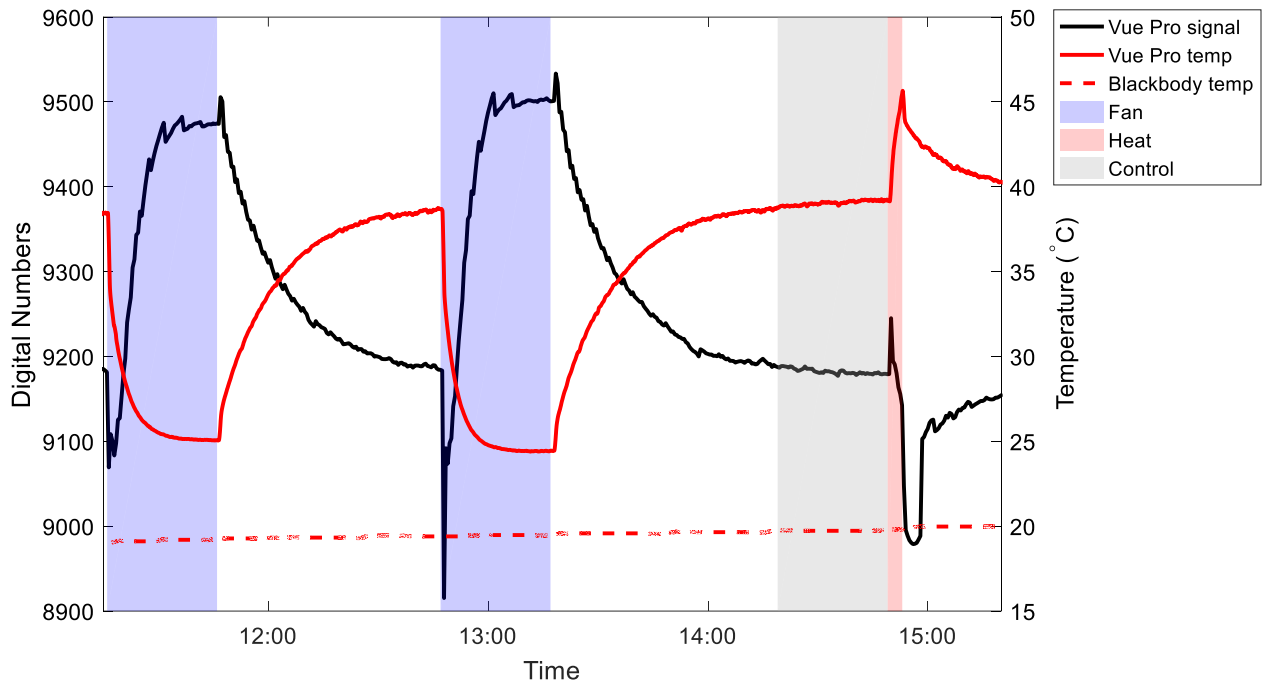

Figure 6. Effect of fan wind and lamp heating on FLIR Vue Pro 640 raw signal (digital numbers). Blue shaded areas indicate fan was switched on. Red shaded area indicates lamp was switched on. Grey shaded area is control period with no wind or heat. No shading (white areas) are camera stabilization periods. Camera signal was stabilized for 1 hour following each fan treatment.

3.1.4   Assessing sensor noise

The results of the experiments so assess sensor noise are shown in Figures 7, 8 and 9. The blackbody radiator was brought close to the camera so that it entirely filled the field of view of the camera. In this way, each pixel in the camera array should have recorded the same temperature.

To test the camera sensor for temporal noise signals, the data were Fourier transformed to produce a plot of power spectral density (Figure 7). The plot shows that on the timescale of seconds (>0.05Hz), there are no significant frequencies contributing to the image signal, whereas at lower frequencies (timescale of minutes) there are appreciable frequency contributions to the signal. These may be partly attributable to the temperature drift of the blackbody (+0.2°C) and camera case (+0.6°C) over the course of the experiment, though these led to only a minor decrease in mean digital number values (-6) between the start and end of the experiment. It is also likely that the camera's internal autocalibration function causes shifts in raw signal every few minutes that contribute to the dominant low frequency signal.
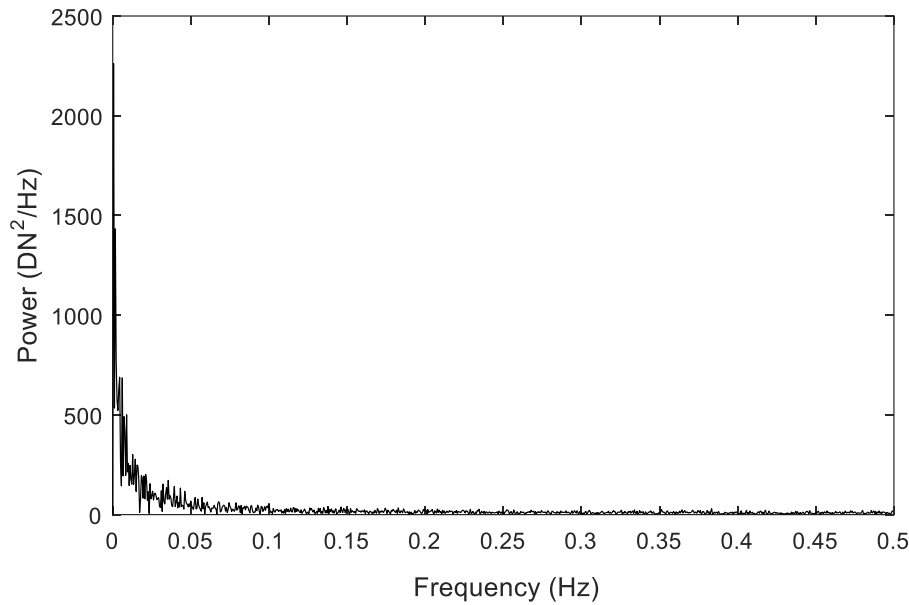
Figure 7. Power density spectrum of mean image digital numbers (DN) from 1800 images captured over 30 minutes of a stable blackbody radiator.

To test for the effects of vignetting, the mean value of individual pixels was compared to the image mean for all images recorded during the experiment (Figure 8). As expected, pixels towards the edge of the sensor record lower than average values, while those towards the centre record higher than average values. Although this effect could be attributed to uneven heat distribution over the surface of the blackbody, a similar effect is noticeable on images captured during UAV flight (Figure 9). The same analysis of vignetting effect was conducted for 10 images captured over a mire ecosystem at the Skogaryd Research Station fieldsite. The lack of large, distinctive features in the mire vegetation enables it to act as a mostly uniform surface (Figure 9a). Pixels in the lower corners of the images are darker than those towards the top (Figure 9b).

Given the small range of values used by the camera, a 1°C temperature change is observed by the camera as a change of ~25 digital numbers (Figure 5). Based on the results in Figure 8, it is possible that the spatial noise across the camera sensor caused by the vignetting effect could cause variability in the range of digital numbers which is >25 digital numbers required to detect a 1°C temperature change. The results imply that the camera is accurate to 2°C.
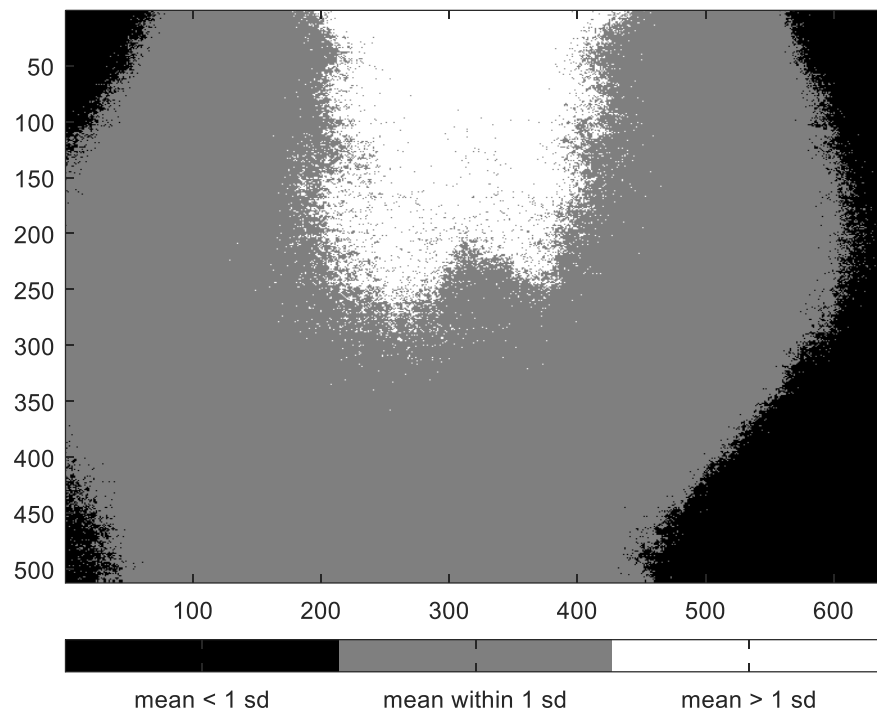
Figure 8. Vignetting effect on the FLIR Vue Pro. Individual pixel means are compared to image mean. Grey pixel means fall within 1σ of the image mean, whilst black and white pixel means are < or > 1σ from the image mean, respectively. Image mean = 9167 digital numbers, σ=8.26 digital numbers.
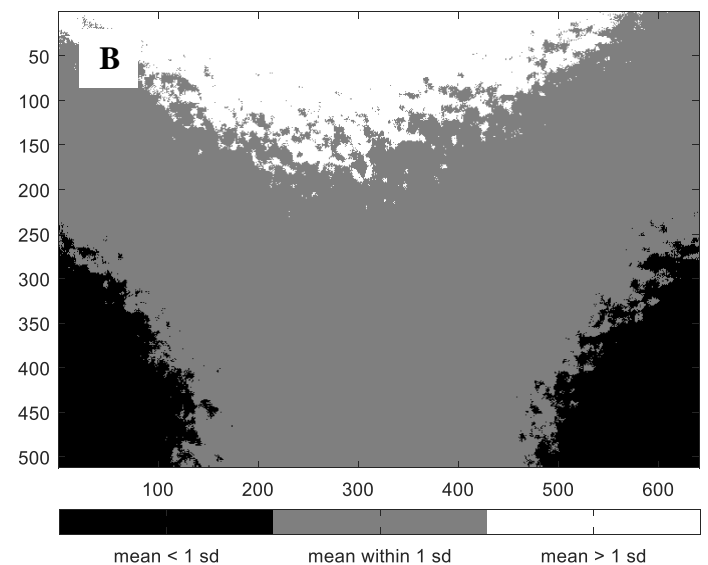

Figure 9. Test for the vignetting effect using 10 images from a UAV flight over a mire ecosystem at the Skogaryd Research Station fieldsite. A) Example image of the mire captured by the FLIR Vue Pro. B) Individual pixel means are compared to the image mean. Grey pixel means fall within 1σ of the image mean, whilst black and white pixel means are < or > 1σ from the image mean, respectively.

Non-uniformity noise, which appears as a pattern of vertical or horizontal stripes is also present on the FLIR Vue Pro sensor (Figure 10). The majority of the correlation coefficients are close to 0, implying these noise patterns have low impact on overall image quality.
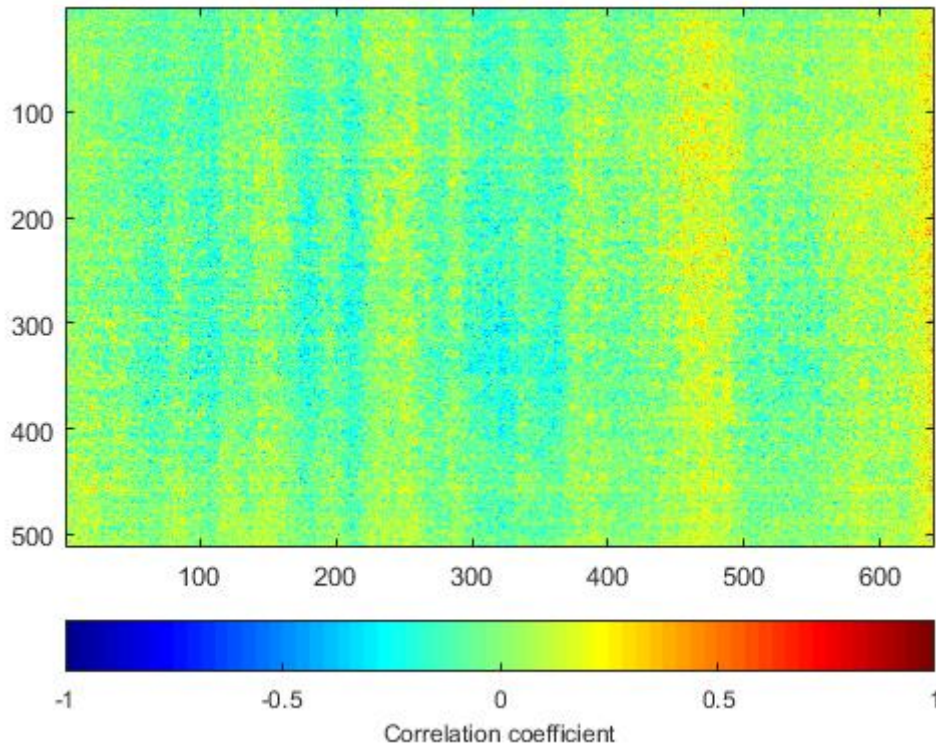

Figure 10. Correlation coefficients between each pixel and the centre pixel.

3.1.5   Geometric calibration of the FLIR Vue Pro 640

Geometric calibration was performed to derive estimates of the intrinsic camera parameters (Table 1). Although the standard error is large on the radial distortion parameters, they should be adequate as an initial input into Agisoft Photoscan Pro which then further refines the estimate when creating an orthomosaic from UAV images. The multispectral and RGB camera were not geometrically calibrated as this information was already available in the image metadata.

Table 1. Intrinsic parameters of FLIR Vue Pro 640 ± standard error. K_{1-3} are radial distortion parameters.

Focal length x (pixels)	812 ± 21.1
Focal length y (pixels)	812 ± 21.2
Principle point x (pixels)	326 ± 2.49
Principle point y (pixels)	255 ± 1.77
K_1	0.07 ± 0.05
K_2	-1.32 ± 0.77
K_3	10.9 ± 4.00

3.1.6   Thermal image processing in Agisoft Photoscan Pro

Unfortunately, generation of an orthomosaic based on the thermal images from a test flight over the fieldsite was not successful due to the low quality of the images. Many of the images

were blurry (a result of the slow shutter speed of the camera in relation to flight speed) and the vignetting effect was also visible on many images. The camera also experienced mechanical problems with the shutter which remained closed while a series of images was taken. Availability of flight data (telemetry data including pitch, yaw and roll) was also essential for correct image alignment. The mire site also contains areas without large clearly defined features (e.g. trees or roads) which renders orthomosaic generation more challenging.

Visit to Skogaryd Research Station and equipment setup design

New equipment to be installed at the field site include permanent ground control points and temperature calibration plates for use with future UAV flights. The design and location of the calibration plates was discussed as well as access to all other data from the site necessary for my PhD research. The location of the new ground-based thermal camera will be adjacent to an existing RBG camera, NDVI and PRI sensors (Figure 5a). The field of view of the thermal camera will thus overlap with these sensors and will view both vegetation zones (wet and dry) present at the site. Future research will investigate variations in the carbon fluxes between these two vegetation zones (Figure 5b). Analyses of the relationships between the carbon fluxes of these vegetation zones and surface temperature, NDVI and PRI measurements from the ground-based sensors will be performed and, where possible, upscaled to the whole mire site using UAV-acquired imagery.

Figure 5a: View of the mire ecosystem and mast where new thermal camera will be installed.

Figure 5b: Example of the wet (blue box) and dry (yellow box) vegetation zones present at the mire site

4. Conclusions and recommendations for future work

The results of the experiments carried out during the STSM revealed that the FLIR Vue Pro 640 thermal infrared camera is sensitive to observed temperature changes of 2°C, accounting for temporal and spatial noise in pixel values. However, the camera temperature measurements are highly dependent on the temperature of the camera itself. Camera temperature is likely to fluctuate during a UAV flight mission as a result of changing wind speeds and solar radiation.

To minimize the effects of these fluctuations on camera temperature measurements, it is recommended to insulate the camera case when mounted on the UAV.

Furthermore, due to the unstable relationship between camera temperature and raw signal, it would be difficult to use the calibration curves generated in the laboratory with the blackbody to derive temperature measurements from images acquired during a UAV flight mission. Instead, it will be necessary to use temperature calibration targets during each UAV flight mission to generate a regression between camera raw signal and observed temperature. The temperature of the panels could be recorded using thermocouples. By placing multiple panels in the field in direct sunlight and in shaded areas, a range of panel temperatures could be captured and thus regressed against digital number values recorded by the FLIR Vue Pro. Using these calibration targets would also account for changes in atmospheric conditions (air temperature, humidity, solar radiation) which would affect the relationship between at-sensor measured radiance and surface temperature.

To enable successful generation of orthomosaics from UAV flight missions, future flights should be performed at a lower flight speed with a greater frontlap and sidelap between images (ideally >80% overlap in both directions). Flying at a lower altitude, and thus increasing the spatial resolution of the images, may also improve feature detection and enable detection of the temperature calibration plates. Image blurriness could be further reduced by installation of a camera mount with vibration compensation or gimbal to reduce camera movement during flight. Furthermore, flight passes to cover the same area from different angles are required in order to minimize the effects of bi-directional reflectance (D. van der Merwe, personal communication, 3 March).

Future collaboration with the host institution (if applicable)

Collaboration is on-going with the host institution as they are providing remote access to the workstation used for processing UAV imagery. Regular communication will be maintained to share knowledge on UAV image processing techniques and updates on the results of future field campaigns using the FLIR Vue Pro and Micasense cameras. The host institution will continue to provide advice on the use of data from the ground-based NDVI and PRI sensors at Skogaryd Research Station.

Forseen publications/articles resulting from the STSM (if applicable)

The results of the laboratory work for radiometric calibration of the FLIR Vue Pro will form the basis of future peer-reviewed publications once sufficient data has been collected with the camera from the Skogaryd Research Station. Furthermore, the work carried out during the STSM will be included as a chapter within my PhD dissertation.

Confirmation by the host institution of the successful execution of the STSM

Attached

References

Aubrecht, D. M.; Helliker, B. R.; Goulden, M. L.; Roberts, D. A.; Still, C. J. & Richardson, A. D. Continuous, long-term, high-frequency thermal imaging of vegetation: Uncertainties and recommended best practices. *Agricultural and Forest Meteorology,* **2016***, 228–229*, 315 - 326

Goodall, T. R.; Bovik, A. C. & Paulter, N. G. Tasking on Natural Statistics of Infrared Images. *IEEE Transactions on Image Processing,* **2016***, 25*, 65-79

Meier, F.; Scherer, D.; Richters, J. & Christen, A. Atmospheric correction of thermal-infrared imagery of the 3-D urban environment acquired in oblique viewing geometry. *Atmospheric Measurement Techniques,* **2011***, 4*, 909-922

Minkina, W. & Dudzik, S. Appendix B: Normal Emissivities of Various Materials (IR-Book 2000, Minkina 2004). Appendix B in *Infrared Thermography, John Wiley & Sons, Ltd,* **2009**, 177-183